# Fourier transform emission spectroscopy of the $C^3\Delta$–$X^3\Phi$, $D^3\Delta$–$X^3\Phi$, $G^3\Phi$–$X^3\Phi$ and $G^3\Phi$–$C^3\Delta$ systems of CoCl

R.S. Ram [a,*], I. Gordon [b], T. Hirao [c], S. Yu [c], P.F. Bernath [a,c,d], B. Pinchemel [e]

[a] *Department of Chemistry, University of Arizona, Tucson, AZ 85721, USA*
[b] *Harverd-Smithsonian Center for Astrophysics, Cambridge, MA 02138, USA*
[c] *Department of Chemistry, University of Waterloo, Waterloo, Ont., Canada N2L 3G1*
[d] *Department of Chemistry, University of York, Heslington, York YO10 5DD, UK*
[e] *Laboratoire PhLAM, Centre d'Etudes et de Recherches Lasers et Applications, Université des Science et Technologies de Lille, 59655 Villeneuve d'Ascq Cedex, France*

## Abstract

The emission spectrum of CoCl has been recorded in the 2000–23 000 cm$^{-1}$ region at high resolution. CoCl was made in a carbon tube furnace by heating cobalt metal to a temperature of about 2300 °C as well as in a DC discharge source and the spectra were observed using a Fourier transform spectrometer. The bands observed in the 2000–13 000 cm$^{-1}$ interval have been classified into four transitions: $C^3\Delta$–$X^3\Phi$ (2500–3600 cm$^{-1}$), $D^3\Delta$–$X^3\Phi$ (9300–10030 cm$^{-1}$), $G^3\Phi$–$X^3\Phi$ (8500–13 000 cm$^{-1}$) and $G^3\Phi$–$C^3\Delta$ (7400–7900 cm$^{-1}$) analogous to the near infrared transitions of CoF reported previously [R.S. Ram, P.F. Bernath, S.P. Davis, J. Chem. Phys. 104 (1996) 6949.]. A rotational analysis of a number of vibrational bands of these transitions has been obtained and spectroscopic constants extracted for the low-lying electronic states of CoCl. It is found that the energy levels of CoCl correlate very well with those of CoF and CoH.
© 2007 Elsevier Inc. All rights reserved.

*Keywords:* Fourier transform spectroscopy; Transition metal halides; Metal chlorides

## 1. Introduction

Transition metal-containing molecules continue to be the focus of recent studies because of their theoretical, chemical and astrophysical importance [1]. A number of these molecules have been investigated in the gas phase and their electronic spectra have been characterized at high resolution. These studies provide insight into chemical bonding in simple metal-containing systems. Because of the high cosmic abundance of transition metal elements in stars, transition metal-containing halides are also of astrophysical importance. The observation of some metal halides such as NaCl, KCl, AlCl and AlF in carbon stars by millimeter-wave astronomers [2,3] strengthens the possi-

bility that transition metal halides may also be found. In spite of this interest the electronic spectra of many transition metal halide molecules remain poorly characterized due to the complexity of their electronic spectra. Because of the presence of d electrons, transition metal-containing molecules have high electronic orbital and electron spin angular momenta. This results in a large number of low-lying electronic states, many of which are high multiplicity states that are further split into sub-states because of large spin–orbit interactions. The electronic transitions in these molecules, therefore, provide complex spectra making their interpretation a challenge. The application of laser excitation and high resolution Fourier transform spectroscopy in recent years has made the analysis of the spectra of many such molecules possible. In some cases high order ab initio calculations have also been found useful in the interpretation of the complex spectra [4–6].

---

Cobalt-containing diatomic halides are good examples for complexity of their electronic spectra. Among the cobalt-containing halides CoF is best characterized while for CoCl only limited studies were available until recently. The CoF molecule has been investigated at high resolution in the visible [7,8], red and near infrared regions [9,10] and submillimeter region [11]. Four electronic transitions, $C^3\Delta$–$X^3\Phi$, $D^3\Delta$–$X^3\Phi$, $G^3\Phi$–$X^3\Phi$ and $G^3\Phi$–$C^3\Delta$ of CoF, involving low-lying electronic states have been observed in the red and near infrared regions [10,11]. By analogy, similar transitions are expected for CoCl, CoBr and CoI.

The spectra of CoCl are known since the 1930s when Mesnage [12] and Moore [13] observed complex bands of CoCl in the visible region using discharge sources. These observations were followed by several low resolution studies [14–16] aimed at the vibrational classification of electronic transitions. The bands were arranged into several electronic transitions, none of which had a lower state vibrational frequency similar to the value of 453.72 cm$^{-1}$ obtained in the matrix isolation observations by Green et al. [17]. Darji et al. [18] analyzed a $\Delta\Omega = 0$ transition of CoCl at 483.4 nm and suggested an $\Omega'' = 0^+$ state as the ground state. A density function theoretical study by Bridgeman [19], however, suggested a $^3\Sigma^-$ ground state. These assignments do not agree with expectations based on results available for CoH [20] and CoF [9,10], which have $X^3\Phi_i$ ground states. Thus the identity of even the ground state of CoCl remained uncertain mainly due to the lack of high resolution data. More recently, Adam et al. [21] reported the observation of two electronic transitions in the 415–725 nm region in a laser-induced fluorescence experiment using laser-ablation/molecular beam source and concluded that the ground state of CoCl indeed arose from a $X^3\Phi_4$ state consistent with the results available for CoF. In a subsequent investigation of CoCl, Hirao et al. [22] recorded the spectrum in same region as studied by Adam et al. [21] and reported additional bands having the $X^3\Phi_3$ spin component of the ground state as the lower state. In another study of this molecule, Wong et al. [23] applied the laser vaporization free jet expansion/laser excitation technique to observe a $^3\Phi_4$–$^3\Phi_4$ subband in the near infrared which they labeled as the [10.3]$^3\Phi$–$X^3\Phi$ transition. Apart from this work, the spectra in the red and near infrared regions remain largely uncharacterized.

In a most recent study of this molecule, Flory et al. [24] measured the pure rotational spectra of CoCl in the ground state by submillimeter-wave spectroscopy. These authors observed pure rotational transitions in the three spin–orbit components with $\Omega = 4$, 3, and 2 of Co$^{35}$Cl and Co$^{37}$Cl establishing the identity of the ground state as $X^3\Phi_i$. From this study they concluded that the molecule is highly perturbed in the ground state.

In the present paper, we report on the high resolution analysis of four transitions of CoCl in the red and near infrared regions. For the [10.3]$^3\Phi$–$X^3\Phi$ transition (relabeled as $G^3\Phi$–$X^3\Phi$ in the present paper) we also observed the $G^3\Phi_3$–$X^3\Phi_3$ component in addition to the $G^3\Phi_4$–$X^3\Phi_4$ subband and

observed bands involving vibrational levels up to $v = 13$ and 9 in the excited $G^3\Phi_4$ and $G^3\Phi_3$ sub-states, respectively. We have also observed three new transitions $C^3\Delta$–$X^3\Phi$, $D^3\Delta$–$X^3\Phi$ and $G^3\Phi$–$C^3\Delta$, in the near infrared. A rotational analysis of numerous bands belonging to the four transitions has been performed and results reported in this paper.

## 2. Experimental

The CoCl molecules were produced using DC discharge and thermal excitation sources. In the first experiment CoCl was produced in the DC discharge in a high temperature tube furnace. A small quantity of CoCl$_2$ powder was placed near the center in a 1.2 m long, 5 cm diameter alumina tube. Two stainless steel sheets were rolled into cylindrical electrodes and placed inside at the ends of the ceramic tubes. The furnace was heated to about 550 °C and a slow flow of Ar gas was used to keep the pressure at about 5 Torr inside the tube. The discharge was generated by operating the DC source at ∼3 kV, 300 mA between the two electrodes. The emission from the source was collected using a CaF$_2$ lens and entered into the entrance aperture of a Bruker IFS 120 HR Fourier transform spectrometer. Spectra in the 8600–23 000 cm$^{-1}$ interval were recorded at a resolution of 0.03 cm$^{-1}$ using a Si-photo diode detector and a photomultiplier tube.

In the second experiment about 40 g of cobalt metal was placed inside King furnace and heated to about 2300 °C. The helium pressure in the furnace was maintained at 150 Torr. A small amount of HCl was introduced into the system at one time, i.e., there was no continuous flow of HCl during the experiment. These conditions have insured the production of CoCl and strong emission signal was imaged onto the entrance aperture of the spectrometer. The spectra in the 1800–22 000 cm$^{-1}$ interval were recorded at a resolution of 0.05 cm$^{-1}$ using InSb and Si-diode detectors.

The line positions were extracted from the observed spectra using a data reduction program called WSpectra developed by M. Carleer (Université Libre de Bruxelles). The branches in the different subbands were sorted using a color Loomis–Wood program running on a PC computer. The measurements of standard Ar atomic lines [25] were used to calibrate the spectra in the 8600–23 000 cm$^{-1}$ region recorded using the high voltage DC discharge source.

In addition to CoCl, the furnace spectra also contained molecular lines of CO, HF and HCl vibration-rotation bands. The lower wavenumber spectra were therefore calibrated using the measurements of HF and HCl [26] while for the higher wavenumber region the Ar calibration was transferred from the high voltage discharge spectra to the furnace spectra using common molecular lines. The absolute accuracy of the wavenumber scale is expected to be of the order of $\pm 0.003$ cm$^{-1}$ for the DC discharge spectra. The CoCl lines of the stronger bands in the King furnace appear with a maximum signal-to-noise ratio of about

twelve and have a typical line width of about 0.08 cm$^{-1}$. Therefore, for the King furnace spectra, the precision of measurements of strong and unblended lines is expected to be of the order of ±0.005 cm$^{-1}$. In the furnace spectra, in particular, several higher vibrational bands (with $v'$ up to 13) were excited and their rotational lines are frequently overlapped with the lines of neighboring bands. The uncertainty of measurements for the weaker and overlapped lines is expected to be much higher than for the cleanly resolved lines.

## 3. Observation and analysis

CoCl has a large number of bands in the 2500–13 000 cm$^{-1}$ region. The lines in the different bands were picked out using a color Loomis–Wood program, which expedited the analysis of bands particularly in complex and overlapped regions. After the branches in the different bands were sorted out, their rotational assignments were made by comparing combination differences from bands having vibrational levels in common. After rotational assignment the spectra in this region have been classified into four transitions: C$^3\Delta$–X$^3\Phi$ (2500–3600 cm$^{-1}$), D$^3\Delta$–X$^3\Phi$ (9300–10030 cm$^{-1}$), G$^3\Phi$–X$^3\Phi$ (8500–13 000 cm$^{-1}$) and G$^3\Phi$–C$^3\Delta$ (7400–7900 cm$^{-1}$). A summary of the observed bands has been provided in Table 1, in which the $T_{00}$ values and 0–0 $R$ heads are also provided for the subbands of each transition. The spectrum in the 8500–13 000 cm$^{-1}$ region is particularly intense and complex because of overlapping from the D$^3\Delta$–X$^3\Phi$ and G$^3\Phi$–X$^3\Phi$ transitions. The D$^3\Delta$–X$^3\Phi$ transition appears with modest intensity while the G$^3\Phi$–X$^3\Phi$ transition is very strong with several sequence bands having vibrational levels up to $v = 5$ in the ground state and $v = 13$ in the upper state.

The general appearance of the near infrared transitions of CoCl are similar to those of CoF as expected, but with

Table 1
Observed near infrared bands of CoCl

| Transition[a] | $T_{00}$ (cm$^{-1}$) | 0–0 $R$ head (cm$^{-1}$) | Observed bands |
|---|---|---|---|
| G$^3\Phi_4$–X$^3\Phi_4$ | 10449.9 | 10051.5 | 0–0, 0–1, 0–2, 0–3, 1–0, 1–4, 1–5, 2–0, 2–5, 3–0, 4–0, 5–1, 6–1, 7–2, 8–2, 9–2, 10–2, 10–3, 10–4, 11–3, 12–4, 13–4, 13–5 |
| G$^3\Phi_3$–X$^3\Phi_3$ | 10486.9 | 10488.5 | 0–0, 0–1, 0–2, 1–0, 1–4, 2–0, 3–0, 4–0, 4–1, 5–1, 6–1, 7–2, 8–2, 9–2, 9–3 |
| C$^3\Delta_3$–X$^3\Phi_4$ | 2726.7 | 2730.6 | 0–0, 1–0, 2–0, 3–1, 4–2, 5–3 |
| C$^3\Delta_2$–X$^3\Phi_3$ | 2636.6 | 2640.6 | 0–0 |
| D$^3\Delta_3$–X$^3\Phi_4$ | 9639.3 | 9637.4 | 0–1, 0–0, 1–0 |
| D$^3\Delta_2$–X$^3\Phi_3$ | 9892.6 | 9894.7 | 0–0 |
| G$^3\Phi_4$–C$^3\Delta_3$ | 7723.2 | 7725.8 | 0–0, 0–1 |
| G$^3\Phi_3$–C$^3\Delta_2$ | 7850.3 | 7853.0 | 0–0 |

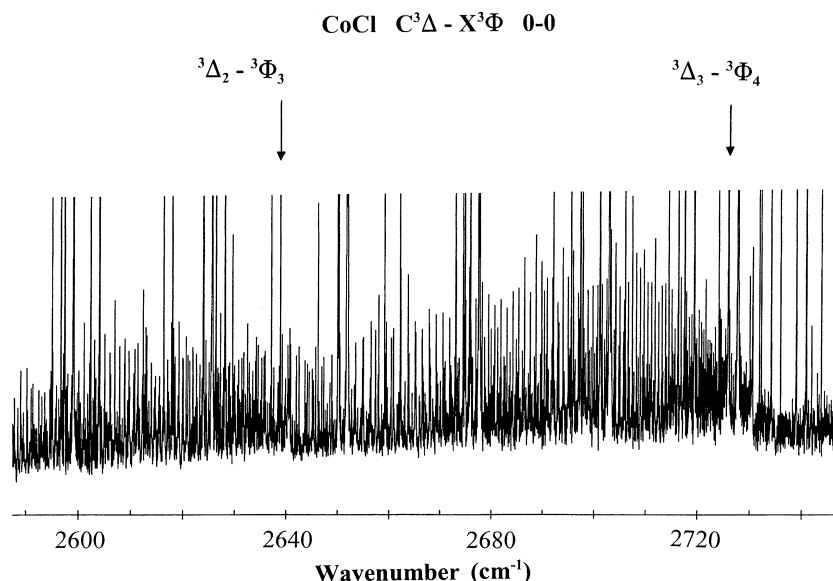[a] Transitions involving the lowest $\Omega$ component of each state were not observed in the spectra.

one exception. Contrary to CoF for which the three spin–orbit components of each state was observed (except D$^3\Delta_1$), the transitions involving the lowest $\Omega$ components (i.e., $\Omega = 2$ for $^3\Phi$ states and $\Omega = 1$ for $^3\Delta$ states) were not observed in our spectra. This could be due to a relatively small population in the lowest $\Omega$ components which lie highest in energy because all the states are inverted, or to interactions with other states. Several additional bands have been observed in the 5000–8500 cm$^{-1}$ and 13 000–20 000 cm$^{-1}$ regions which still remain unassigned because of their very weak intensity and complexity. Some of these bands could be due to singlet states.

The chlorine atom has two isotopes $^{35}$Cl and $^{37}$Cl with a natural abundance ratio of about 3:1, therefore spectra of both isotopologues, Co$^{35}$Cl and Co$^{37}$Cl, are expected to be present in our spectra. It was found that rotational lines belonging to the minor isotopologue Co$^{37}$Cl are generally overlapped with the strong lines of other bands located in the same region. This is particularly true for the $\Delta v > 0$ sequence bands where the minor isotopologue bands fall on the lower wavenumber side of the main isotopologue and are overlapped by much stronger lines of the main isotopologue of the same band. However, lines belonging to the minor isotopologue are clearly identified in the $\Delta v < 0$ bands, particularly for the first member of the sequence since Co$^{37}$Cl heads are located on the higher wavenumber side of the Co$^{35}$Cl heads and are not overlapped by the strong Co$^{35}$Cl lines.

### 3.1. The C$^3\Delta$–X$^3\Phi$ transition in the 2500–4500 cm$^{-1}$ region

Seven bands belonging to this transition are located in the 2500–3600 cm$^{-1}$ region. After rotational analysis, two bands with origins near 2727 and 2636 cm$^{-1}$ have been assigned as the 0–0 bands of the C$^3\Delta_3$–X$^3\Phi_4$ and C$^3\Delta_2$–X$^3\Phi_3$ subbands; the C$^3\Delta_1$–X$^3\Phi_2$ subband was not observed in spite of a careful search. Only the $v = 0$ vibrational level of the C$^3\Delta_2$ spin component was observed in our spectra since the $^3\Delta_2$–$^3\Phi_3$ subband is weaker than the $^3\Delta_3$–$^3\Phi_4$ subband. In addition to the 0–0 band, five additional bands with origins near 3130, 3531, 3498, 3467 and 3436 cm$^{-1}$ have been identified as the 1–0, 2–0, 3–1, 4–2 and 5–3 bands (respectively) of the $^3\Delta_3$–$^3\Phi_4$ subband. No $\Omega$-doubling was resolved in the assigned $J$ range in contrast to the large $\Omega$-doubling observed in the C$^3\Delta$ state of CoF. The observed bands consist of $P$, $Q$ and $R$ branches with the $Q$ branch being the most intense. This observation is consistent with a $\Delta\Omega = -1$ assignment for these bands. The rotational lines in these bands do not have combination defects or $\Omega$-doubling, suggesting that high $\Omega$ states ($\Omega > 1$) must be involved. The rotational lines show no hyperfine splittings in the range of observed $J$ values, although some broadening has been observed for very low $J$ lines. The $\Omega$-assignment for the two subbands has been made by comparing the lower state constants with the values reported in previous studies. A compressed portion containing the 0–0 bands of the two subbands is

**CoCl  C³Δ - X³Φ  0-0**



Fig. 1. A compressed portion of the C³Δ–X³Φ transition of CoCl with the 0–0 heads of the ³Δ₂–³Φ₃ and ³Δ₃–³Φ₄ subbands marked.

presented in Fig. 1. The spectrum of this transition is overlapped by very strong molecular lines belonging to HCl and CO. It was noted that the lower $J$ lines of the fundamental HCl band appear as broad absorption features which obscure many CoCl molecular lines. Because of overlapping as well as weaker intensity the bands belonging to $\Delta v = -1$ and $-2$ sequences could not be identified. Rotational lines as high as $R(97)$, $P(99)$, $Q(99)$ and $R(144)$, $P(118)$, $Q(158)$ were observed in the 0–0 bands of the C³Δ₂–X³Φ₃ and C³Δ₃–X³Φ₄ subbands, respectively. No local perturbations were observed in any of the bands belonging to this transition.

### 3.2. The D³Δ–X³Φ transition in the 9300–9900 cm⁻¹ region

Four bands with $R$ heads near 9209, 9639, 9893 and 10 027 cm⁻¹ have been attributed to another ³Δ–³Φ electronic transition of CoCl. These bands are weaker than the overlapping bands of the G³Φ–X³Φ transition present in the same region. The band at 9893 cm⁻¹ has been assigned as the 0–0 band of the D³Δ₂–X³Φ₃ subband. No other bands belonging to this subband were identified in our spectra probably due to their very weak intensity. The bands located near 9209, 9639 and 10 027 cm⁻¹ have been assigned as the 0–1, 0–0 and 1–0 bands of the D³Δ₃–X³Φ₄ subband. Another band located near 9216 cm⁻¹ has been assigned as the 0–1 band of the D³Δ₃–X³Φ₄ subband of the Co³⁷Cl isotopologue. Like the C³Δ–X³Φ transition, these bands also consist of $R$, $Q$ and $P$ branches, consistent with a $\Delta\Omega = -1$ assignment. These bands are free of Ω-doubling suggesting that high Ω value (Ω > 1) states are involved. A part of the 0–0 band of the D³Δ₃–X³Φ₄ subband at 9639 cm⁻¹ is presented in Fig. 2. The lower wavenumber side of this band is overlapped with a the 1–3 band of the G³Φ₃–X³Φ₃ subband

located near 9593 cm⁻¹. The rotational lines of the different branches have, therefore, not been marked in this figure to avoid confusion.

### 3.3. The G³Φ–X³Φ transition in the 8500–13 000 cm⁻¹ region

A very intense transition of CoCl has been observed in the 8500–13 000 cm⁻¹ region. Two bands located at 10 450 and 10 487 cm⁻¹ have been assigned as the 0–0 bands of the ³Φ₄–³Φ₄ and ³Φ₃–³Φ₃ subbands of the G³Φ–X³Φ transition. The spectrum consists of several sequences of bands and each sequence consists of many higher vibrational bands. In total we have identified 23 bands involving vibrational levels $v' = 0$–13 and $v'' = 0$–5 for the ³Φ₄–³Φ₄ subband and 15 bands involving vibrational levels $v' = 0$–9 and $v'' = 0$–4 for the ³Φ₃–³Φ₃ subband. A search for bands belonging to the ³Φ₂–³Φ₂ subband as well as cross-spin component transitions with $\Delta\Omega \neq 0$ was not successful. A part of the compressed spectrum of this transition is provided in Fig. 3 with some of the main sequence bands marked, although the sequence structure is wider than shown in this figure. For example, we have identified bands up to 1–5 in the $\Delta v = -4$ sequence and 13–5 in the $\Delta v = 8$ sequence of the ³Φ₄–³Φ₄ subband. A part of the 1–0 band near the $R$ heads is provided in Fig. 4 where bands belonging to the ³Φ₃–³Φ₃ and ³Φ₄–³Φ₄ subbands have been marked. Each band belonging to this transition consists of only $R$ and $P$ branches as expected for a $\Delta\Omega = 0$ transition. An expanded portion of the G³Φ₃–X³Φ₃ 1–0 band is provided in Fig. 5 in which some low $J$ $R$ and $P$ lines have been marked. We have identified rotational lines up to $R(138)$ and $P(128)$ in the G³Φ₃–X³Φ₃ subband and $R(90)$ and $P(90)$ in the corresponding G³Φ₄–X³Φ₄ subband.

A part of the spectrum of the 0–1 band near the $R$ heads have been provided in Fig. 6 in which the $R$ heads of both iso-
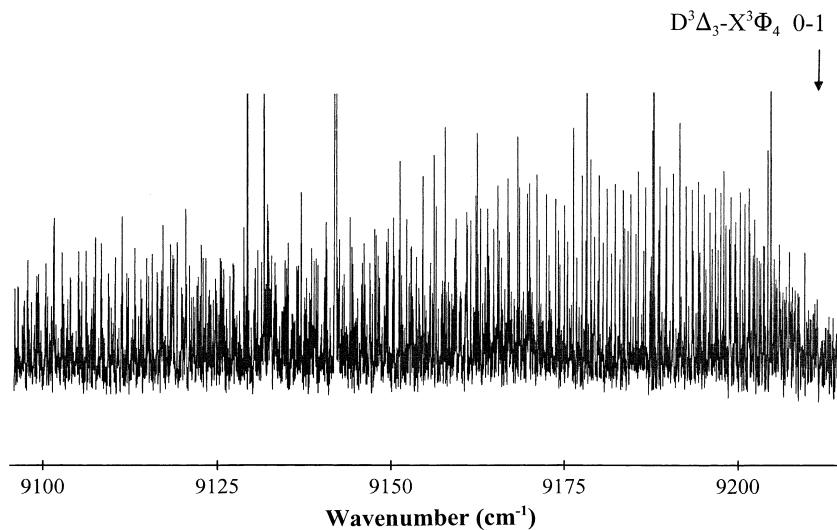
Fig. 2. A portion of the $D^3\Delta_3$–$X^3\Phi_4$ 0–0 band of CoCl. The individual rotational lines have not been marked to avoid confusion.
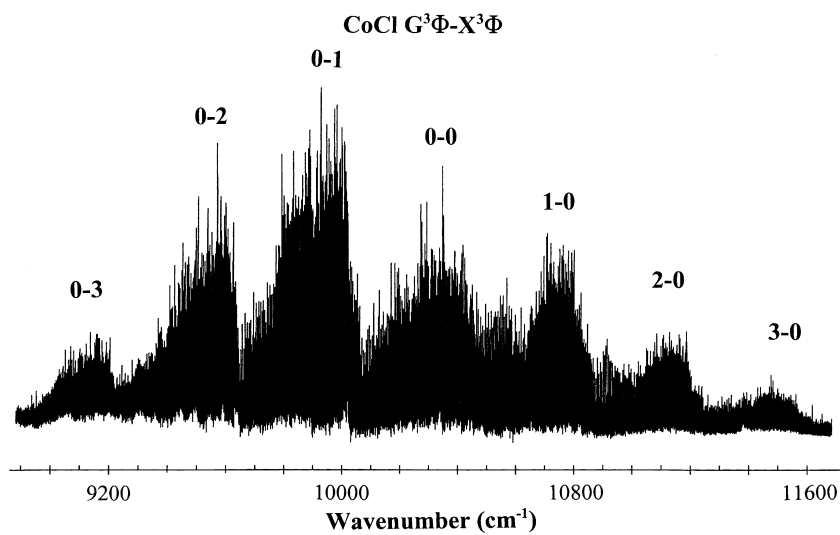


Fig. 3. An overview of the $G^3\Phi$–$X^3\Phi$ transition of CoCl with the main sequence bands marked.
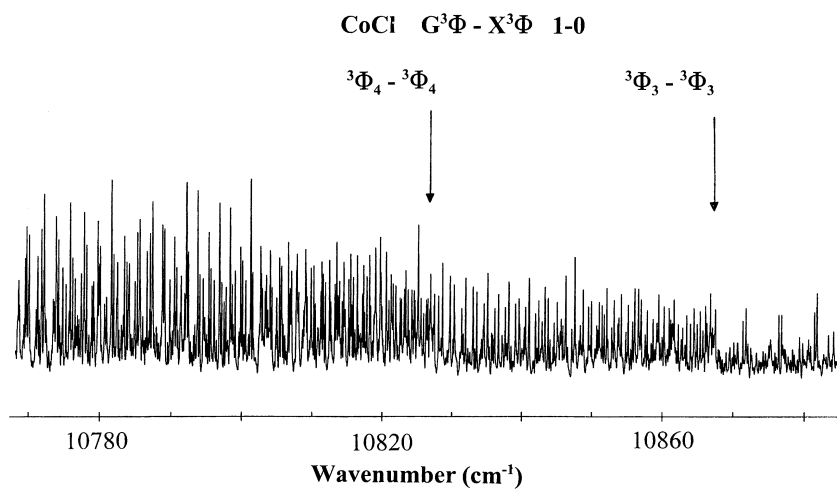


Fig. 4. A portion of the 1–0 band of the $G^3\Phi$–$X^3\Phi$ system of CoCl near the band heads. The $R$ heads of the $^3\Phi_3$–$^3\Phi_3$ and $^3\Phi_4$–$^3\Phi_4$ subbands have been marked.
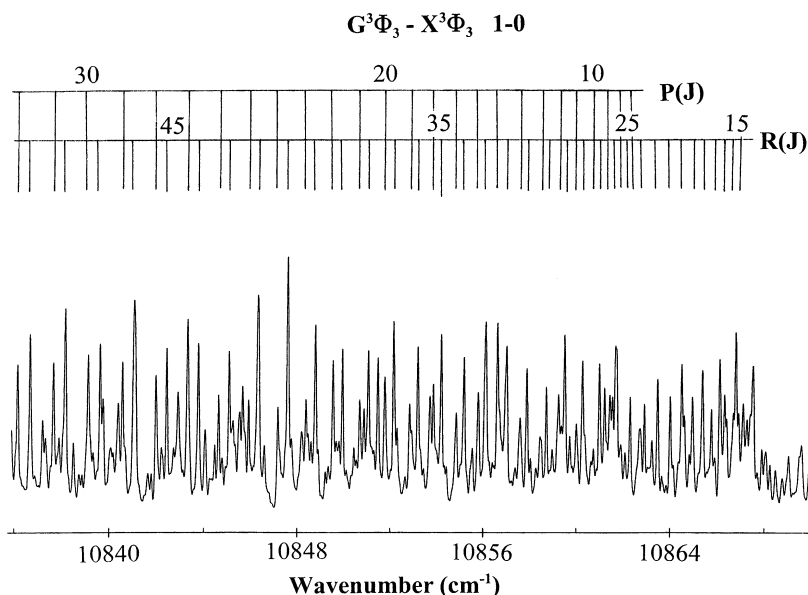
$G^3\Phi_3$ - $X^3\Phi_3$   1-0



Fig. 5. An expanded portion of the 1–0 band of the $G^3\Phi_3$–$X^3\Phi_3$ subband with some low $J$, $R$ and $P$ lines marked near the band head.
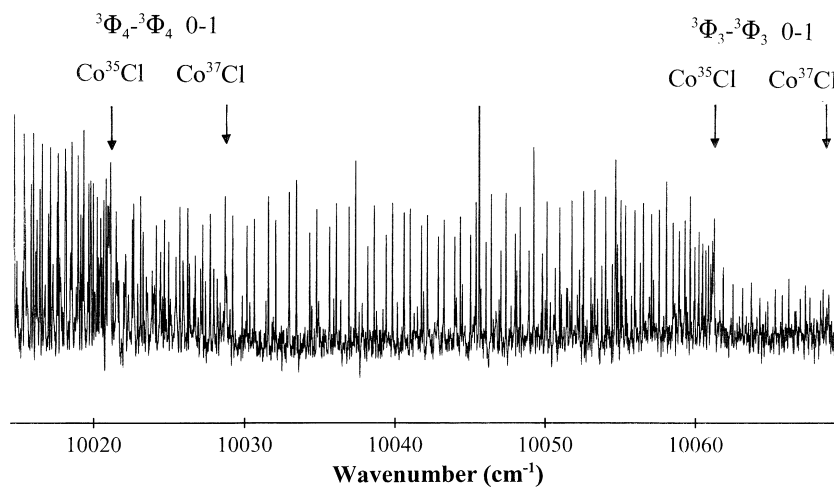


Fig. 6. A portion of the 0–1 band of the $G^3\Phi$–$X^3\Phi$ transition of the CoCl with the $R$ heads of the $Co^{35}Cl$ and $Co^{37}Cl$ isotopologues marked.

topologues have been marked. No attempt was made to rotationally analyze $Co^{37}Cl$ bands because of the limited data available. In this work, therefore, we have obtained spectroscopic constants only for the main isotopologue $Co^{35}Cl$.

### 3.4. The $G^3\Phi$–$C^3\Delta$ transition in the 7400–7900 cm$^{-1}$ region

Some weaker bands observed in the 7000–7900 cm$^{-1}$ region have been attributed to the $G^3\Phi$–$C^3\Delta$ transition of CoCl. Two bands located near 7723 and 7850 cm$^{-1}$ have been identified as the 0–0 bands of the $G^3\Phi_4$–$C^3\Delta_3$ and $G^3\Phi_3$–$C^3\Delta_2$ subbands. The $G^3\Phi_4$–$C^3\Delta_3$ 0–0 band position was calculated simply by taking the difference of the band origins of the $G^3\Phi_4$–$X^3\Phi_4$ 0–0 and $C^3\Delta_3$–$X^3\Phi_4$ 0–0 bands (10449.9 − 2726.7 = 7723.2 cm$^{-1}$) and rotational lines were easily found in our spectra using the Loomis–Wood program, in spite of its weak intensity. Similarly the

$G^3\Phi_3$–$C^3\Delta_2$ 0–0 band position was calculated by taking the difference of the $G^3\Phi_3$–$X^3\Phi_3$ 0–0 and $C^3\Delta_2$–$X^3\Phi_3$ 0–0 bands. The third $G^3\Phi_2$–$C^3\Delta_1$ subband of this transition was again not identified in our spectra as discussed previously.

No attempt was made to obtain a Hund's case (a) fit of the observed lines due to the lack of satellite branches that cross-spin components ($\Delta\Sigma \neq 0$ transitions). The molecular constants for the different $\Omega$ states were therefore determined separately by fitting the observed line positions to the customary empirical energy level expression:

$$F(J) = T_v + B_v J(J + 1) - D_v[J(J + 1)]^2 + H_v[J(J + 1)]^3$$
$$+ L_v[J(J + 1)]^4.$$

The $\Omega$-doubling constants are omitted in this expression as the $\Omega$-doubling was not resolved in any bands over the ob-

Table 2
Spectroscopic constants[a] (in $cm^{-1}$) for the $X^3\Phi$ state of CoCl

| State | $v$ | $T_v$ | $B_v$ | $10^7 \times D_v$ |
|---|---|---|---|---|
| $X^3\Phi_3$ | 0 | 0.0 | 0.1793156(27) | 1.2649(22) |
| | 1 | 427.4154(12) | 0.1783218(27) | 1.2700(23) |
| | 2 | 851.3104(14) | 0.1773139(28) | 1.2890(24) |
| | 3 | 1271.7065(47) | 0.1759163(46) | 1.2655(64) |
| | 4 | 1688.5527(20) | 0.1754744(33) | 1.3190(46) |
| $X^3\Phi_4$ | 0 | 0.0 | 0.17954254(22) | 1.24939(80) |
| | 1 | 430.45048(92) | 0.17857747(45) | 1.24873(85) |
| | 2 | 857.5853(12) | 0.17761593(65) | 1.2495(10) |
| | 3 | 1281.4215(57) | 0.1766589(33) | 1.2542(41) |
| | 4 | 1701.9459(46) | 0.1757272(30) | 1.2920(40) |
| | 5 | 2119.2490(64) | 0.1747651(38) | 1.2896(47) |

[a] The numbers in parentheses are one standard deviation in the last two digits quoted.

Table 3
Spectroscopic constants[a] (in $cm^{-1}$) for the $C^3\Delta$ and $D^3\Delta$ states of CoCl

| State | $v$ | $T_v$ | $B_v$ | $10^7 \times D_v$ |
|---|---|---|---|---|
| $C^3\Delta_2$ | 0 | 2636.57400(89) | 0.1719502(27) | 1.2289(22) |
| $C^3\Delta_3$ | 0 | 2726.73386(56) | 0.17166200(26) | 1.23113(80) |
| | 1 | 3130.0620(14) | 0.17075567(92) | 1.2244(14) |
| | 2 | 3530.7094(27) | 0.1698586(13) | 1.2202(15) |
| | 3 | 3928.7199(19) | 0.16896318(79) | 1.21083(97) |
| | 4 | 4324.0965(16) | 0.16808116(84) | 1.2050(11) |
| | 5 | 4716.8969(59) | 0.1672019(34) | 1.1995(41) |
| $D^3\Delta_2$ | 0 | 9892.6314(66) | 0.1663255(28) | 1.0497(24) |
| $D^3\Delta_3$ | 0 | 9639.3612(10) | 0.16626532(45) | 1.19784(85) |
| | 1 | 10027.0072(10) | 0.1653601(14) | 1.1128(43) |

[a] The numbers in parentheses are one standard deviation in the last two digits quoted.

Table 4
Spectroscopic constants[a] (in $cm^{-1}$) for the $G^3\Phi$ state of CoCl

| State | $v$ | $T_v$ | $B_v$ | $10^7 \times D_v$ | $10^{11} \times H_v$ | $10^{15} \times L_v$ |
|---|---|---|---|---|---|---|
| $G^3\Phi_3$ | 0 | 10486.96406(83) | 0.1616211(27) | 1.1622(22) | — | — |
| | 1 | 10866.01822(97) | 0.1607893(27) | 1.1658(23) | — | — |
| | 2 | 11242.4289(12) | 0.1599663(30) | 1.1863(34) | — | — |
| | 3 | 11616.2802(14) | 0.1591213(28) | 1.1532(24) | — | — |
| | 4 | 11987.4618(17) | 0.1582779(28) | 1.1298(24) | — | — |
| | 5 | 12356.0200(26) | 0.1574680(42) | 1.149(11) | 0.0123(97) | — |
| | 6 | 12721.9667(41) | 0.1566489(59) | 1.204(19) | 0.097(18) | — |
| | 7 | 13085.2521(58) | 0.1558536(97) | 1.289(41) | 0.198(53) | — |
| | 8 | 13445.9281(59) | 0.1550485(74) | 1.338(23) | 0.187(21) | — |
| | 9 | 13804.0294(28) | 0.1541639(33) | 1.1260(34) | — | — |
| $G^3\Phi_4$ | 0 | 10449.93762(93) | 0.1612555(13) | 1.0536(56) | −0.2097(89) | 0.1675(46) |
| | 1 | 10826.0540(14) | 0.1604294(29) | 0.940(16) | −0.478(30) | 0.523(19) |
| | 2 | 11199.4993(20) | 0.1596386(41) | 0.815(23) | −0.670(48) | 1.020(33) |
| | 3 | 11570.2655(15) | 0.1589157(34) | 0.980(21) | 0.331(46) | 0.699(33) |
| | 4 | 11938.3724(17) | 0.1582278(31) | 0.802(14) | 1.405(18) | — |
| | 5 | 12303.8447(36) | 0.157642(10) | 0.250(85) | 3.20(26) | −3.00(27) |
| | 6 | 12666.6439(33) | 0.1573321(58) | −2.117(28) | −2.423(39) | — |
| | 7 | 13023.0684(31) | 0.1553417(15) | 1.1535(20) | 0.00348(56) | — |
| | 8 | 13382.875(15) | 0.153429(18) | −1.225(75) | −2.70(12) | 1.201(70) |
| | 9 | 13738.6143(11) | 0.152382(13) | −1.290(47) | −2.406(70) | 0.914(35) |
| | 10 | 14091.3066(61) | 0.1514089(85) | −1.679(40) | −3.171(75) | 1.419(48) |
| | 11 | 14440.840(13) | 0.150946(11) | 0.050(26) | −0.587(19) | — |
| | 12 | 14788.025(11) | 0.150014(13) | −0.517(52) | −1.535(79) | 0.567(40) |
| | 13 | 15132.4241(65) | 0.1492437(72) | −0.285(29) | −1.307(46) | 0.496(24) |

[a] The numbers in parentheses are one standard deviation in the last two digits quoted.

served $J$ range. In the final fit, the blended and weaker lines were given lower weights depending on their signal-to-noise ratio and extent of blending. The hyperfine-free line frequencies of the pure rotational transitions observed by Flory et al. [24] were also included in the final fit with appropriate weights. The lines of the bands in the four transitions are available from the Journal depository. The rotational constants for the $X^3\Phi$ state are provided in Table 2 while the constants for the $C^3\Delta$ and $D^3\Delta$ states are provided in Table 3. The spectroscopic constants for the $G^3\Phi$ state obtained from the final fit are provided in Table 4.

## 4. Discussion

Although several visible transitions of CoCl have been studied at high resolution previously [21,22], the red and near infrared regions remained largely unexplored: only the $^3\Phi_4$–$^3\Phi_4$ subband of the $G^3\Phi$–$X^3\Phi$ transition was observed previously by Wong et al. [23]. In that work the authors observed the $v = 0$ the vibrational level in the $X^3\Phi_4$ state and $v = 2$–7 vibrational levels in the $G^3\Phi_4$ spin component [labeled by them as $[10.3]^3\Phi_4$]. No other low-lying electronic states have been observed in previous studies. Based on the similarity of the electronic structure of CoF and CoH [9,10], two low lying $^3\Delta$ states are expected below the $G^3\Phi$ state of CoCl and we have located $C^3\Delta$ and $D^3\Delta$ states in the work reported here. The energy levels of the low-lying electronic states of CoCl based on the present work have been compared with those of CoF and CoH in the
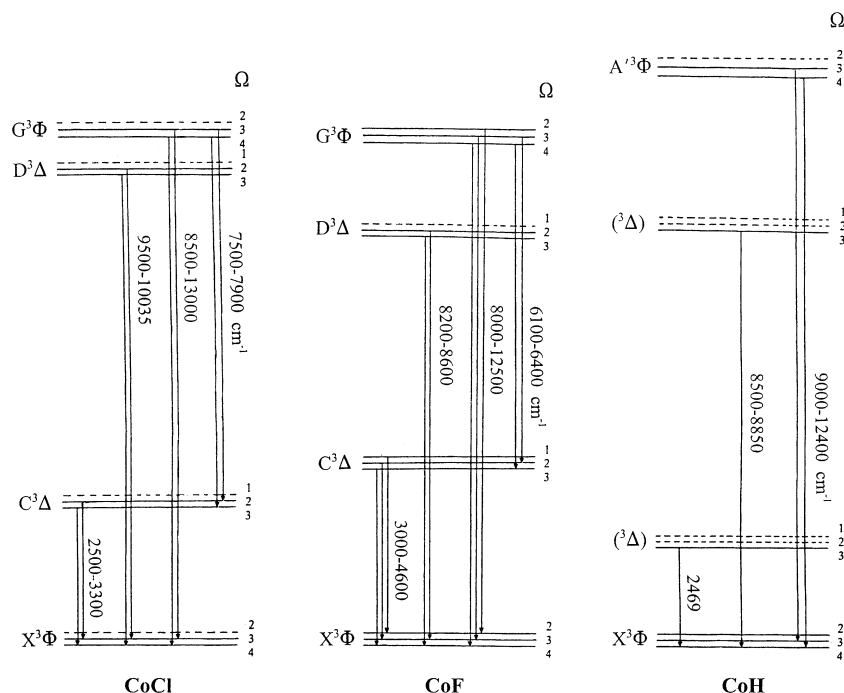
Fig. 7. An schematic energy level diagram of the observed low-lying electronic states of CoCl, CoF and CoH. A good correspondence exists between the observed electronic states of the three molecules, as expected.

energy level diagram provided in Fig. 7. From this figure it can be concluded that the electronic structure and ordering of the states are indeed very similar.

The spectroscopic constants for the ground states (Table 2) agree very well with the values reported by Hirao et al. [22] and Wong et al. [23], but are more precise and extensive compared to the previous value. While comparing the constants we noticed some typos in Table 2 of Hirao et al. [22]. The labeling of the spin–orbit components of the $X^3\Phi$ state should be $\Omega = 4$ and 3 instead of $\Omega = 3$ and 2, respectively. The spectroscopic constants for the observed states reported in Tables 2–4 indicate that the $X^3\Phi$, $C^3\Delta$ and $D^3\Delta$ states are relatively free from perturbation because the constants vary in a regular manner. This is not the case for the $G^3\Phi$ state where an irregular variation is observed in the rotational constants. This is especially true for the $G^3\Phi_4$ spin component where higher order $H_v$ and $L_v$ constants are needed for most of the vibrational levels. The vibrational levels with $v' > 5$ also have abnormal (and some times negative) values for the distortion constants, which means that these levels are affected by interactions with other close-lying states (or state). The rotational constants as well as the vibrational intervals for the affected states also vary in an erratic manner. For example the values for $\Delta G_{1/2}$ (376.1164 cm$^{-1}$), $\Delta G_{3/2}$ (373.4453 cm$^{-1}$), $\Delta G_{5/2}$ (370.7662 cm$^{-1}$), $\Delta G_{7/2}$ (368.1069 cm$^{-1}$), $\Delta G_{9/2}$ (365.4723 cm$^{-1}$) and $\Delta G_{11/2}$ (362.7992 cm$^{-1}$) vary in a more or less a regular manner as expected, while the values for $\Delta G_{13/2}$ (356.4245 cm$^{-1}$), $\Delta G_{15/2}$ (359.7884 cm$^{-1}$), $\Delta G_{17/2}$ (355.7573 cm$^{-1}$), $\Delta G_{19/2}$ (352.6923 cm$^{-1}$), $\Delta G_{21/2}$ (349.5334 cm$^{-1}$), $\Delta G_{23/2}$

Table 5
Equilibrium constants (in cm$^{-1}$) for the low-lying electronic states of CoCl

| Constants | $X^3\Phi_4$ | $X^3\Phi_3$ | $C^3\Delta_3$ |
|---|---|---|---|
| $B_e$ | 0.1800272(23) | 0.179771(44) | 0.1721064(53) |
| $\alpha_e$ | 0.0009616(20) | 0.000964(18) | 0.0008961(20) |
| $\omega_e$ | 433.787(12) | 430.9323(44) | 405.973(11) |
| $\omega_e x_e$ | 1.6722(63) | 1.75879(93) | 1.3267(24) |
| $\omega_e y_e$ | 0.00283(84) | — | — |
| $r_e$(Å) | 2.065599(13) | 2.06707(25) | 2.112597(33) |
| | $D^3\Delta_3$ | $G^3\Phi_4$ | $G^3\Phi_3$ |
| $B_e$ | 0.16671792(87) | 0.161807(92) | 0.1620277(86) |
| $\alpha_e$ | 0.0009052(15) | 0.000907(27) | 0.0008279(18) |
| $\omega_e$ | [387.6460(14)]$^a$ | 378.7909(38) | 381.6819(63) |
| $\omega_e x_e$ | — | 1.33998(95) | 1.31184(74) |
| $\omega_e y_e$ | — | 0.000845(53) | — |
| $r_e$(Å) | 2.1464658(56) | 2.17880(62) | 2.177311(58) |

$^a$ $\Delta G_{1/2}$ value.

(347.1850 cm$^{-1}$) and $\Delta G_{25/2}$ (344.3991 cm$^{-1}$), have an erratic variation with increasing $v$ values. The constants of Tables 2–4 have been used to determine the equilibrium constants for the different states if more than one vibrational level has been observed. The values for the levels affected by interactions have been given reduced weights. The equilibrium constants for the different spin components were determined separately and are provided in Table 5.

## 5. Conclusion

We have recorded the emission spectrum of CoCl in the 1800–23 000 cm$^{-1}$ region using a Fourier transform spec-

trometer. The bands observed in the 2000–13 000 cm$^{-1}$ range have been assigned to four electronic transitions: $C^3\Delta$–$X^3\Phi$, $D^3\Delta$–$X^3\Phi$, $G^3\Phi$–$X^3\Phi$ and $G^3\Phi$–$C^3\Delta$. The spectroscopic constants of the new low-lying electronic states have been determined through rotational analysis. The assignment of the $X^3\Phi$ state as the ground state of CoCl is consistent with the results available for the isovalent CoF and CoH molecules [9,10] and supported by the observation of pure rotational transitions. The $v > 4$ vibrational levels of the $G^3\Phi_4$ spin component are affected by interactions with some unknown electronic states. No spectra involving the lowest $\Omega$ component of the four observed states have been detected.

## Acknowledgments

## Appendix A. Supplementary data

Supplementary data associated with this article can be found, in the online version, at doi:10.1016/j.jms.2007.03.007.

## References

[1] C. Jascheck, M. Jascheck, The Behaviour of Chemical Elements in Stars, Cambridge University Press, Cambridge, 1995.
[2] J. Cernicharo, M. Guélin, Astron. Astrophys. 183 (1987) L10–L12.
[3] L.M. Ziurys, A.J. Apponi, T.G. Phillips, Astrophys. J. 433 (1994) 729–732.
[4] R.S. Ram, A.G. Adam, A. Tsouli, J. Liévin, P.F. Bernath, J. Mol. Spectrosc. 186 (1997) 113–130.
[5] R.S. Ram, N. Rinskopf, J. Liévin, P.F. Bernath, J. Mol. Spectrosc. 1228 (2004) 544–553.
[6] R.S. Ram, P.F. Bernath, S.P. Davis, J. Chem. Phys. 116 (2002) 7035–7039.
[7] A.G. Adam, Chem. Phys. Lett. 230 (1994) 82.
[8] A.G. Adam, W.D. Hamilton, J. Mol. Spectrosc. 206 (2001) 139.
[9] R.S. Ram, P.F. Bernath, S.P. Davis, J. Mol. Spectrosc. 173 (1995) 158.
[10] R.S. Ram, P.F. Bernath, S.P. Davis, J. Chem. Phys. 104 (1996) 6949.
[11] T. Okabayashi, M. Tanimoto, J. Mol. Spectrosc. 221 (2003) 149–155.
[12] P. Mesnage, C. R. Acad. Sci. 201 (1935) 389–391.
[13] K.R. Moore, Phys. Rev. 54 (1938) 122–125.
[14] V.G. Krishnamurty, Indian J. Phys. 26 (1952) 177–185.
[15] S.V.K. Rao, P.T. Rao, Indian J. Phys. 35 (1961) 556–561.
[16] C.V. Reddy, A.L. Narayana, P.T. Rao, Opt. Pura Appl. 17 (1984) 289–296.
[17] D.W. Green, D.P. McDermott, A. Bergman, J. Mol. Spectrosc. 98 (1983) 111–124.
[18] A.B. Darji, M.B.S. Kumar, N.R. Shah, P.M. Shah, Indian J. Pure Appl. Phys. 26 (1988) 44–46.
[19] A.J. Bridgeman, J. Chem. Soc. Dalton Trans. (1997) 4765–4772.
[20] M. Freindorf, C.M. Marian, B.A. Hess, J. Chem. Phys. 99 (1993) 1215–1223.
[21] A.G. Adam, J.R.D. Peers, Y. Tang, C. Linton, J. Mol. Spectrosc. 221 (2003) 149–155.
[22] T. Hirao, B. Pinchemel, P.F. Bernath, J. Mol. Spectrosc. 219 (2003) 119–128.
[23] A.L. Wong, W.S. Tam, A.S.-C. Cheung, J. Chem. Phys. 119 (2003) 3234–3239.
[24] M.A. Flory, D.T. Halfen, L.M. Ziurys, J. Chem. Phys. 121 (2004) 8385–8392.
[25] G. Norlén, Phys. Scripta 8 (1973) 249–268.
[26] R.B. Le Blanc, J.B. White, P.F. Bernath, J. Mol. Spectrosc. 164 (1994) 574–579.